Molecular dynamics studies of granular flow through an aperture

D. Hirshfeld, Y. Radzyner, and D. C. Rapaport
Physics Department, Bar-Ilan University, Ramat-Gan 52900, Israel
(Received 25 November 1996; revised manuscript received 23 May 1997)

Molecular dynamics methods are used to study two-dimensional gravity-driven granular flow through a horizontal aperture. Two distinct approaches to modeling the granular particles are studied. (a) Circular particles subject to a strongly repulsive short-range interaction, together with normal and tangential frictional damping forces. (b) Rigid nonconvex particles, each consisting of disks arranged as an equilateral triangle, suitably spaced to provide a tangible indentation along each edge; the same repulsive interactions between disks in different grains and normal frictional damping forces are incorporated, but transverse damping is omitted, with the model relying on grain shape to resist sliding motion. In order to allow accurate measurements under steady-state conditions, a continuous-feed approach is adopted, in which grains exiting through the hole are returned to the top of the material in the container. For both models the output flow is measured as a function of aperture size, and the observed behavior is compared with previous theoretical and experimental results. Tests of the degree to which the models reproduce the depth independence of the flow are reported, and the influence of the container width and the nature of the walls are studied. The depth dependence of the pressure, the local stress distribution, and the particle flow patterns are also examined.
[S1063-651X(97)05710-3]

PACS number(s): 83.70.Fn, 02.70.Ns, 46.10.+z, 05.60.+w

I. INTRODUCTION

There is a clear need to develop the capability to predict the qualitative and quantitative flow behavior of dry granular materials under the variety of conditions that arise in industrial applications. In contrast to atomistic systems, for which atomic theory, equilibrium statistical mechanics, and linear response theory provide the theoretical underpinnings for numerical many-body studies aimed at elucidating the detailed mechanisms of fluid flow, the far more complex behavior displayed by granular materials lacks any established theoretical foundation, and the problem must therefore be addressed by an *a priori* numerical approach. The aim of such numerical studies is to determine how interparticle interactions, boundary effects, and gravitational forces combine to produce effects observed in, for example, flow through apertures (as in hopper flow), flow along inclined surfaces (chute flow), and convection and size segregation under vertical vibration, to name but a few of the phenomena that are both of scientific interest and great industrial importance.

Computer modeling plays an important role in the effort to understand the nature of granular matter. The observation that much of what characterizes granular flow is universal, in the sense that substances of very different constituency exhibit common behavior, is an indication that it ought to be possible to determine which of the underlying properties of the individual grains bear primary responsibility for the qualitative nature of the behavior, and which play only a secondary role and determine the quantitative details. Since, from a computational point of view, the present state of our understanding of the nature of granular matter makes it impossible to represent the full complexity of granular materials, the decision as to how the key features should be represented allows some freedom of choice. Only through careful comparison between simulation and experiment—and so far very few attempts have been made at the sufficiently detailed level necessary to probe the stresses and motion correlations of individual grains—will it be possible to decide which of the models provides the most faithful representation of granular substances.

The most detailed approach available for investigating problems of granular flow is based on the molecular (or granular) dynamics simulation of systems of inelastic particles. In this paper we report on a detailed study of the flow of granular material through a horizontal aperture. For computational convenience the system studied is two dimensional. Two distinct models for granular particles are investigated—the motivation for examining alternative models is to determine the extent to which general features of the behavior are independent of the details of the model. In the first of these models the particles are represented as disks that interact with one another through strong repulsive forces that prevent overlap, as well as normal and tangential damping forces that provide the energy dissipation and shear resistance characteristic of a variety of granular substances. In the second model the grains are represented as rigid triangular assemblies of disks that are subject to normal damping forces only; here the absence of tangential damping should at least be partly compensated for by the more complex granular shape whose concavities inhibit sliding under a normal load. To obtain the long runs and steady flow state necessary to provide adequate statistics, we introduce a scheme for recycling grains as they exit through the aperture. We examine the extent to which the measured behavior agrees with experimental observations, and also compare our results with previous related work.

II. BACKGROUND

The last few years have witnessed numerous attempts at using particle-level modeling [1,2] in order to simulate a variety of granular flows [3] in full detail. Much of the work

has concentrated on the somewhat intriguing problem of size-dependent segregation under vibration, but other key problems, such as shear flow and flow through an aperture, have also been addressed. In some respects simulation now leads experiment: the kinds of detailed measurements probing the properties of both individual grains and small groups of grains that are readily accomplished in the course of a simulation have only recently attracted the attention of experimentalists [4]. While many aspects of simulation and experiment are found to be in broad agreement at the bulk level, a full validation of the granular models used in the simulations will eventually require a detailed comparison of stresses and dynamic correlations at the level of individual grains. The fact that simulation is able to reproduce some of the features of granular flow is, of course, insufficient to establish that other properties are adequately represented.

This paper addresses the problem of gravity-driven flow of granular material through a horizontal aperture, a simplified model for the outflow from a silo or storage tank with vertical walls. This is clearly a problem of considerable industrial importance, but engineering design is based on a continuous-medium treatment [5] that completely ignores the discrete nature of the grains. In the present study, both for computational convenience and following the prevailing tradition of most granular simulations carried out to date, the problem is treated in two dimensions; this is not expected to lead to any substantial differences in the behavior, beyond those of a geometric nature associated with the change of dimensionality.

There have been two previous related studies of this problem reported in the literature, in which disklike grains were permitted a single pass through the aperture [6,7]. This kind of approach limits the duration of the computer experiment and prevents the attainment of a time-independent steady state, where measurements of behavior can be made that are sufficiently accurate to be used in comparisons between different models and parameter settings. The present work overcomes this difficulty by employing a continuous-feed mechanism; this is accomplished by replacing each grain exiting through the aperture by a new grain that is introduced near the upper surface of the bulk in a manner that maintains an almost flat surface profile.

Numerous experiments have been made in the past with the aim of relating the flow rate to the aperture size [8]. These have led to a number of empirical observations that determine which parameters of the problem actually influence flow rate: (a) The flow rate is independent of the material height (or head) H, provided this is more than 2.5 times the width W of the containing cylinder; this is the reason an hourglass—where a constant mean flow rate is an essential characteristic—is able to function properly. (b) The flow rate is independent of W if this is greater than 2.5 times the aperture size D, and also exceeds $D+30d$, where d is the typical grain diameter. (c) Provided the granular material is not too fine, the flow proceeds relatively smoothly for $D>6d$; blockage tends to occur when $D<4d$.

Given that the only parameters remaining to determine the flow are the aperture size D and the gravitational constant g, dimensional analysis [5] predicts (subject to an implicit assumption that D is not too large) that the discharge rate (or mass flux) in three dimensions is proportional to $g^{1/2}D^{5/2}$. If allowance is made for the fact that, because of the finite grain size, the effective aperture size is not D but $D-kd$, where kd is the size of the so-called empty annulus, and k is a number that must be determined experimentally for each kind of material [9], then the discharge rate should be

$$\frac{dN}{dt}=C\rho g^{1/2}(D-kd)^{5/2}, \tag{1}$$

where ρ is the grain packing density near the aperture, and C is a constant that also depends on the material type. Such a formula has achieved considerable success in fitting the measured discharge rates for a wide range of granular substances [8,9], typically to within about 5%. In many cases k lies in the range 1.3–1.5, although the typical value for sand turns out to be $k=2.9$.

There is at least one plausible physical explanation for the result derived via dimensional analysis [8]. Since the flow is dominated by the behavior in the vicinity of the aperture, it seems appropriate to introduce the concept of a free-fall arch; above the arch grains are packed together and mutually impede each other's motion, with the result that flow is retarded. Below the arch the grains are essentially unconfined, the stress is zero, and so they accelerate freely under the influence of gravity. If the characteristic arch size is that of the aperture itself then, irrespective of the precise shape of the arch, the general result follows (although more detailed descriptions have been proposed [10]). This behavior should be contrasted with the outflow of a simple liquid, where the now height-dependent discharge rate is proportional to $(gH)^{1/2}D^2$.

The simulations described here involve the two-dimensional version of the problem. The same dimensional considerations apply, leading to an expression for the discharge rate

$$\frac{dN}{dt}=C\rho g^{1/2}(D-kd)^{3/2}. \tag{2}$$

One of the principal results of this paper will be a detailed numerical test of this formula for the models of granular materials introduced in Sec. III.

III. COMPUTATIONAL MODEL

A. Granular interactions

Simple inspection reveals the structural complexity of granular matter. The grains themselves are irregularly shaped, sometimes covered with asperities, and are normally polydisperse. The collisions between grains are highly inelastic; frictional forces of some kind are essential, because in their absence it would be difficult for the material to form piles; the wear-and-tear of collisions can even alter the shape of the grains to some extent. Which of these (and other) characteristics must be incorporated into the model in order to reproduce particular aspects of the observed behavior can only be established by extensive testing.

Applications of molecular dynamics simulation to studies of matter at the atomistic scale involve potentials based on well-defined theoretical and experimental considerations. The state of affairs in granular modeling is very different,

due to the irregular shapes of the granular particles and the highly complex nature of the forces between them. Consequently, the detailed information required to achieve a level of understanding of the nature of the individual granular particles adequate for the development of a simulational program is more empirical in nature. What is in fact needed is a simplified representation of the salient features of the grain geometry and the interactions; detailed comparisons between simulations, more elaborate theoretical models, and actual experiment can then be used to establish how good an approximation has been achieved [11,12].

Models presently in use are typically based on inelastically colliding soft [13,14] or hard [15] spheres (or disks for two-dimensional simulations), more often the former; rotational motion of individual particles may or may not be included in the dynamics. Normal and tangential velocity-dependent (viscous) damping forces are introduced to represent the inelasticity of the collisions and the surface roughness. Static friction is difficult to model, but its effect can at least be partially represented by a force that resists sliding motion while grains are in contact, which, for a soft-sphere model, means whenever the grains are within interaction range.

Since real grains tend to be irregularly shaped, it would seem obvious that this property should be included in the model. More elaborate models involving nonspherical particles that have been introduced for various kinds of granular simulations, as part of the effort to reproduce the correct behavior include rigid [16] or flexible [17] assemblies of spheres, elliptical grains [18], and more complex structures formed of elastic triangles linked by deformable damped beams [19] that permit the modeling of grains with sharp corners. As the level of detail increases so does the computational effort, and it is important to have some way of assessing which features of the model are actually responsible for the observed behavior. An example of this is the comparative importance of friction and particle geometry [17]; to some extent, nonconvex grains can compensate for the lack of static friction since they are able to mutually interlock with one another, but the degree to which this is able to account for the effects attributed to friction still awaits clarification.

1. Circular particles

One of the two models considered here is based on monodisperse circular grains. The interaction that prevents overlap when grains collide is assumed—with a modicum of arbitrariness—to have the Lennard-Jones (LJ) form, with a cutoff at the point where the repulsive force is exactly zero,

$$\boldsymbol{f}_{ij}^{r}=\frac{48\epsilon}{r_{ij}}\left[\left(\frac{\sigma}{r_{ij}}\right)^{12}-\frac{1}{2}\left(\frac{\sigma}{r_{ij}}\right)^{6}\right]\hat{\boldsymbol{r}}_{ij}, \tag{3}$$

for grains located at $\boldsymbol{r}_i$ and $\boldsymbol{r}_j$, where $\boldsymbol{r}_{ij}=\boldsymbol{r}_i-\boldsymbol{r}_j$, and $r_{ij}=|\boldsymbol{r}_{ij}|$. Here ϵ and σ define suitable energy and length scales; both can be set to unity without loss of generality since the results can be converted into any desired system of physical units. The interaction cutoff occurs at $r_{ij}=r_c=2^{1/6}\sigma$; thus the grain diameter, although not precisely defined because the interaction strength drops smoothly to zero, is of order r_c. The LJ interaction is strongly repulsive at small distances, more so than the linear overlap or Hertzian type (overlap to the $\frac{3}{2}$ power) repulsions often used in granular simulations, and only a small degree of mutual grain penetration can occur. Thus the grains might be considered harder, though less so than for a $1/r^{36}$ interaction employed in a study related to the present work [7]. How much hardness is required to achieve grainlike behavior is also a question that has no obvious answer; it is worth pointing out, however, that if the range of separations over which interaction occurs is made too narrow, the efficacy of the damping and/or frictional forces used to inhibit shearing becomes questionable.

In addition to this short-range repulsion there are viscous damping forces [13,14] that act in both the normal and transverse directions whenever the grain separation is below r_c. The normal component is

$$\boldsymbol{f}_{ij}^{n}=-\gamma_n\dot{\boldsymbol{r}}_{ij}\cdot\hat{\boldsymbol{r}}_{ij}, \tag{4}$$

where γ_n is the normal damping coefficient. The transverse (or sliding) component of the damping force is

$$\boldsymbol{f}_{ij}^{s}=-\mathrm{sgn}(v_{ij}^{s})\min(\mu|f_{ij}^{r}+f_{ij}^{n}|,\gamma_s|v_{ij}^{s}|)\hat{\boldsymbol{s}}_{ij}, \tag{5}$$

where

$$v_{ij}^{s}=\dot{\boldsymbol{r}}_{ij}\cdot\hat{\boldsymbol{s}}_{ij}+\tfrac{1}{2}r_{ij}(\omega_i+\omega_j) \tag{6}$$

is the relative tangential velocity of the disks at their closest point, $\hat{\boldsymbol{s}}_{ij}=\hat{z}\times\hat{\boldsymbol{r}}_{ij}$ is a unit vector tangential to the disks at this point ($\hat{z}$ is a unit vector pointing out of the plane of the system), ω_i and ω_j are the angular velocities of the disks, and γ_s is the transverse damping coefficient. The static friction coefficient μ appears as part of an upper bound imposed on the transverse force due to the Coulomb criterion. Numerical values for the various parameters are given below.

In this ansatz, both the normal and transverse damping forces share responsibility for energy dissipation; the transverse force also inhibits sliding motion, although not rolling motion. There is no static friction force in this model; some simulations include a term of this kind [7,13,14] based on a simple spring model, but while, as mentioned earlier, this type of interaction is required to stabilize static or near-static configurations (even though a spring mechanism does not offer the same degree of shear resistance as static friction at low shear rates), it has yet to be determined whether it has any significant effect on flowing systems such as those treated here. If the results described later in this paper are compared with those of Ref. [7], it even appears that the contrary is true: spring-based friction does not make the flowing material significantly more granular. From a recent critical discussion [12] of the variety of force laws used in simulating granular flow, it emerges that much remains to be done insofar as accurately modeling granular particles is concerned (an examination of the restitution coefficient for head-on collisions using the LJ repulsive interaction reveals a slight increase with velocity, a trend similar to the more widely used linear-overlap force). Nevertheless, despite the oversimplification involved, empirical models of the kind used here—with assorted minor variations—have proved themselves successful in a wide range of contexts.

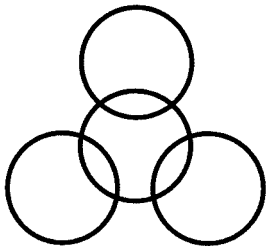

FIG. 1. The shape of the triangular grain drawn to scale; the diameter of the particle is arbitrarily defined to be that of the circumcircle.

2. Triangular particles

Granular particles that are not entirely convex provide an appealing extension of the basic spherical (or circular) grain model since, at least to a limited extent, the potentially interlocking shapes imitate the behavior caused by the asperities on rough, irregularly shaped grains. The concavities have the ability to inhibit sliding because a packed cluster of grains must dilate before shearing motion can begin. In a sense, this should provide partial compensation for the absence of explicit static friction from the model, and possibly even serve as a more realistic model for granular matter than those based on springs and viscous damping mechanisms. The second of the two models studied in the present paper is of this kind.

Each grain—as shown in Fig. 1—consists of three disks fixed at the vertices of an equilateral triangle; the disks are positioned sufficiently far apart for a significant indentation to occur along each edge, and a fourth disk is placed at the centroid of the triangle to fill the central void that would otherwise occur. The forces between these rigid triangular particles are based on the same Lennard-Jones repulsion, Eq. (3), used to prevent overlap of circular particles, but now acting between pairs of disks in different grains, where each coordinate $\boldsymbol{r}_i$ now represents the location of one of the disks that make up the grain. Energy dissipation is provided by the same normal velocity-dependent viscous damping between individual pairs of disks introduced previously. Unlike the model based on circular grains, however, we do not include any transverse damping, but rely on geometrical effects to supply the required transverse motion inhibition necessary to prevent grains sliding over one another.

B. Boundary conditions

Boundaries are an essential component of any granular simulation and, as with the granular interactions themselves, a simplified representation must be adopted. Real walls are rough and tend to inhibit sliding motion. Such walls can, for example, be represented by stochastic boundaries, which absorb energy and reflect each grain with a much reduced speed in a random direction, or as granular boundaries constructed out of disks whose positions are fixed along the boundary plane (or line) with spacing chosen sufficiently large to achieve the effect of a corrugated wall, but not so large that grains can penetrate the wall when subjected to high stress. Granular boundaries can also include mixed disk sizes and variable spacing, both of which are intended to reduce any tendency for the material to form ordered layers. An unphysical, elastic boundary consists of a frictionless wall with which grains undergo energy-conserving specular collisions without any change in angular velocity; this can be useful in cases where the sole purpose is to prevent grains from leaving the simulation region. In certain cases, if the nature of the problem warrants this, it might even be appropriate to use periodic boundaries.

Most of the work reported here is based on uniformly spaced granular walls, with the boundary disks having the same characteristics as those of the bulk (as used in the circular grain model). For the circular grains the distance between the disks forming the container base is 0.5σ and the distance between disks in the vertical walls is σ; for triangular grains the spacing of the disks along each of the walls is set to r_c. A range of possible values could be used, subject to the spacing being adequate to inhibit flow and not overly encourage the bulk material to pack as a lattice (the latter particularly important for the horizontal base). During the initial phase of the simulation the aperture is blocked by additional boundary grains, but when the moment in the simulation is reached for flow to commence, the disks forming the plug are removed.

C. Continuous flow mechanism

To achieve the continuous flow conditions necessary for a prolonged period of steady-state flow, grains exiting through the hole are removed from the system and reintroduced at suitable locations just above the surface of the bulk material. A grain is considered to have passed through the hole when its center of mass falls below the level of the container base, but recycling does not take place until the grain has dropped a distance of two grain diameters below this level; this allows it to continue to interact for a short time with any grains following closely behind. This approach not only allows repeatable flow measurements, but ensures a constant head of material throughout the measurement period, thereby eliminating possible height-dependent effects, while at the same time requiring only a relatively small system.

The grain recycling mechanism has to be constructed in a way that avoids any unwanted perturbation of the material flow. The horizontal position of each reintroduced grain is therefore picked to be at the lowest accessible point on the upper surface of the material, the height is chosen to be slightly above the grains lying immediately below this position (determined by dividing the system into a series of vertical strips and locating the highest grain in each), and the velocity is set to an initial downward value similar in magnitude to the outflow velocity. This method ensures that the top surface remains almost flat, and avoids the central depression that might otherwise develop. Such an approach appears to have a negligible effect on the flow, especially when the material head is much greater than the hole size, as is the case here. An alternative approach to recycling, based on adding an entire layer at once (but which does not place special emphasis on ensuring a horizontal upper surface), has been used for studying flow in a hopper with sloping walls [20].

D. Computational details

In the case of circular grains, once the form of the normal and tangential forces acting on each of the disks has been

decided upon, the translational and rotational equations of motion follow immediately. For the triangular grains, given the forces acting between all pairs of disks, the net forces and torques on the grains can be computed. In computing the torques, the overlap force is regarded as acting between the disk centers; the normal damping is considered to act at the midpoint of the line between the disk centers, which, assuming only a small amount of overlap is allowed by the repulsive overlap force, is essentially the point of contact of the disks. The rotational equation of motion that must be solved is just the two-dimensional version of the Euler equation

$$\dot{\omega}_i = N_i / I, \tag{7}$$

where ω_i is the angular velocity of grain i, N_i the total torque acting on the grain, and I the moment of inertia about the center of mass.

The present formulation uses reduced (or dimensionless) units, following standard practice in molecular dynamics (MD). For circular grains, the (approximate) grain diameter r_c is defined as the unit of length, while for triangular grains, because of the difficulty in designating an effective diameter, the unit of length is set to σ. The energy scale is specified by choosing the coefficient ϵ of the LJ repulsion to be unity as well. Determining the system of units is completed by setting the particle mass to unity for the circular grains, and likewise for the masses of the individual disks that form the triangular grain. In terms of these units the integration time step is $\Delta t = 10^{-3}$; this particular value of Δt is chosen so that in the absence of damping the numerical solution achieves a satisfactory degree of energy conservation.

For a particular set of force definitions the measured properties will of course depend on the values of the parameters that determine the interactions. For circular grains, the values $\mu = 0.5$, $\gamma_n = 100$, and $\gamma_s = 100$ are used; while the damping forces should be as large as possible in order to enhance the inelasticity of the grains, they must be kept small enough to avoid the occurrence of numerical instability while integrating the equations of motion. Over a reasonable range of values the behavior does not appear to be particularly sensitive to small changes in these damping constants. The gravitational acceleration is set to $g = 10$.

For triangular grains the spacing between disks along the edge of each grain is chosen to be $1.6 r_c$ (so that the grain diameter $d = 2.84 r_c$); this ensures a shape with a degree of concavity that is able to significantly inhibit sliding motion when grains are pushed together. It is also a value at which the measured head dependence of the discharge rate appears to be relatively small; this dependence cannot be eliminated entirely, as will be shown below. The other parameters used in this case are $\gamma_n = 2$ and $g = 1$.

The initial state is constructed of grains with random positions and velocities (and random orientations in the case of triangular grains). Before opening the hole (which is initially blocked by additional boundary grains) the grains are allowed to fall freely (a viscous damping force can be temporarily included to prevent excessive velocity buildup during this phase), and eventually form a relatively close-packed configuration from which practically all kinetic energy has been dissipated. After the hole is opened measurements are made at regular intervals over blocks of 10^4 time steps, and the results then averaged over a series of ten such blocks to produce the final averages and standard deviations.

The standard neighbor list method [21] is used to reduce the overall computational effort to a level that is proportional to the number of grains (rather than one that grows quadratically with system size). The coupled equations of motion are integrated numerically using the leapfrog method in the case of circular grains and a fourth-order predictor-corrector method for the triangular grains.

IV. RESULTS

A. Continuous flow discharge rate

The first series of measurements deals with the flow rate as a function of aperture size, for a fixed container width and material head. Experimental measurements and theoretical predictions for this most prominent property of the flow were discussed earlier; it is clearly important to see whether the granular material modeled here is able to reproduce the expected behavior.

1. Circular grains

The measurements of flow rate for the model based on circular grains involve a system with $N = 3000$ grains, and a container width $W = 50$. Note that all lengths are expressed in terms of the approximate grain diameter r_c (or unity in reduced units), and this will henceforth be denoted by the quantity d. The size of the hole ranges from $D = 2$ to 18. The number of grains passing through the hole per unit time is measured as a function of time, as are the vertical and horizontal mean velocity components of the exiting grains. The total number of grains exiting through the hole during the course of the run depends on D and the total run length, and typically lies in the range $5-50\times10^3$, but since many of the grains—particularly those close to the container sidewalls—experience very little motion, the implication is that the grains actively participating in the flow make several passes through the system.

In Fig. 2 we plot the discharge rate (or particle flux) dN/dt as a function of hole size D, and show the results of a simple least-squares fit to the predicted [9] $\frac{3}{2}$ power law in Eq. (2). The value of k, the parameter defining the width of the empty annulus, is determined from the fit to be 2.2, not too far from the values quoted experimentally. The smallest values of D, namely, $D \leqslant 5$, are not included in the fit; experimentally the power law is only claimed to be accurate for D values that are at least five times the grain diameter d. The simulation results are very close to the theoretical curve; if anything, they are in closer agreement than experiment, although given the technical difficulties encountered in performing a precisely controlled real experiment this is perhaps not surprising. The fact that the behavior is grainlike rather than liquidlike (which would imply a linear dependence on D) points to the success of the model in capturing this particular aspect of the behavior. A similar dependence on hole size [7] has been obtained for a model that includes a spring-based (transverse) frictional interaction, but the present results suggest that the additional forces could well be irrelevant—at least in the context of the particular model in which they were used (further evidence to support this statement appears later).

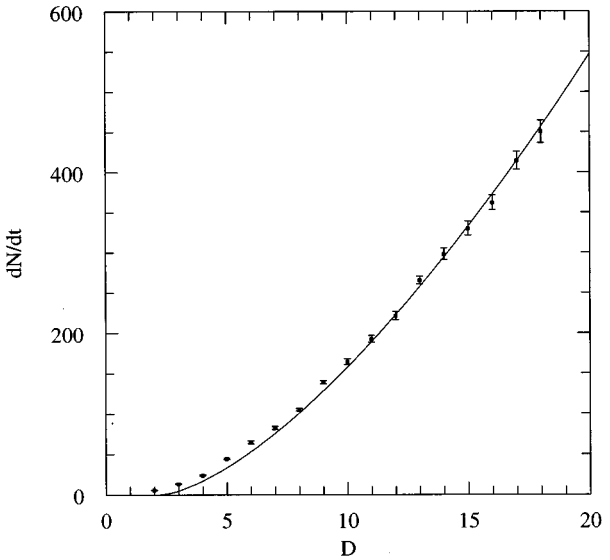

FIG. 2. Particle flux as a function of hole size (in reduced units) for circular particles; the fit shown is to the theoretically predicted curve $dN/dt \propto (D-kd)^{3/2}$.

Figure 3 shows the vertical velocity v_y of the exiting grains as a function of the hole size. The fit to the expected square-root dependence on $(D-kd)$—this is simply the flux divided by the effective aperture size—is also shown, using the same value of k as in the previous fit. The horizontal exit-velocity results (based on the averaged absolute value $|v_x|$), for which there are no theoretical results or measurements available, are shown in Fig. 4; a linear fit seems appropriate here for $D>5$, and this is included, but without any attempt at justification.

2. Triangular grains

The flow measurements for triangular particles are based on a system of $N=7800$ granular particles. The container

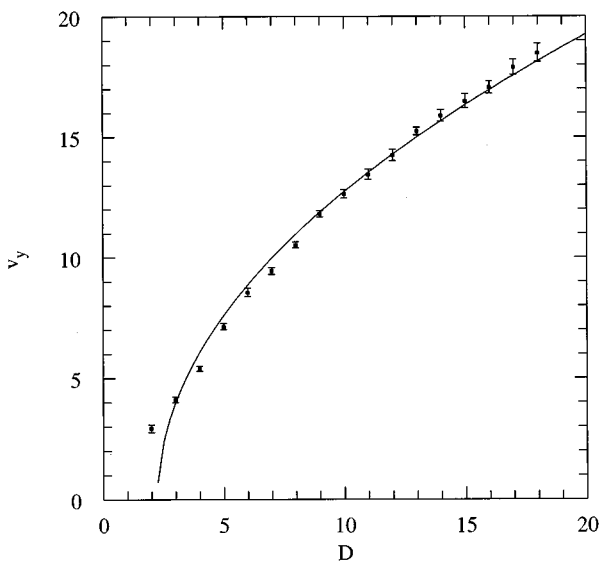

FIG. 3. Vertical outflow velocity as a function of hole size for circular particles; the fit is to the curve $v_y \propto (D-kd)^{1/2}$ using the same value of k as before.

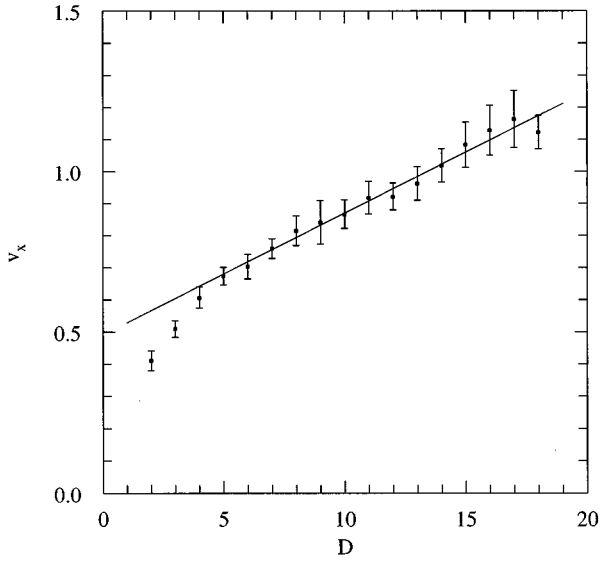

FIG. 4. Horizontal outflow velocity as a function of hole size (circular particles); a linear fit is included.

width W is chosen to be a factor of 5 greater than the largest value of the hole size D considered; as will be demonstrated below (for circular grains), the walls are then sufficiently far away for neither the precise value of W, nor the nature of the walls, to affect the flow. Given W, the number of particles is then chosen to be large enough (within reason) to reduce the height dependence of the flux as much as possible—examination of the residual dependence on height is described below.

Figure 5 shows the dependence of discharge rate on D, with a fit to the $\frac{3}{2}$ power law [Eq. (2)]. The agreement is of similar quality to the circular grains; the error bars here are larger, both because the results are based on a smaller number of grains traversing the hole over the course of the run and because the flow fluctuations are inherently larger. The

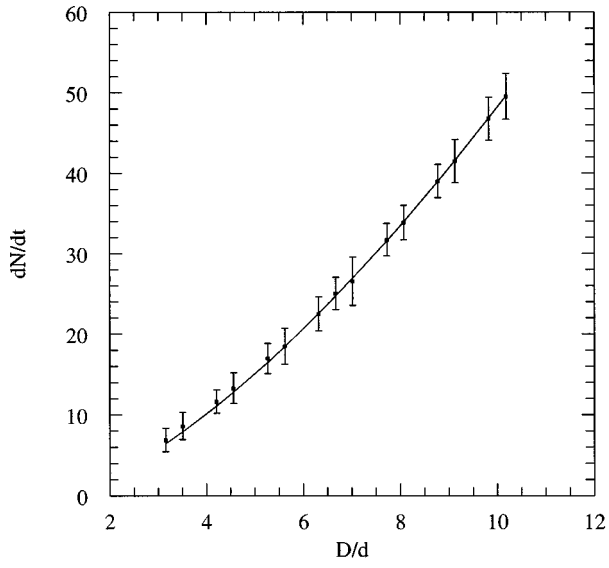

FIG. 5. Particle flux as a function of hole size (expressed in terms of the grain diameter d) for triangular particles; the theoretical fit is shown.

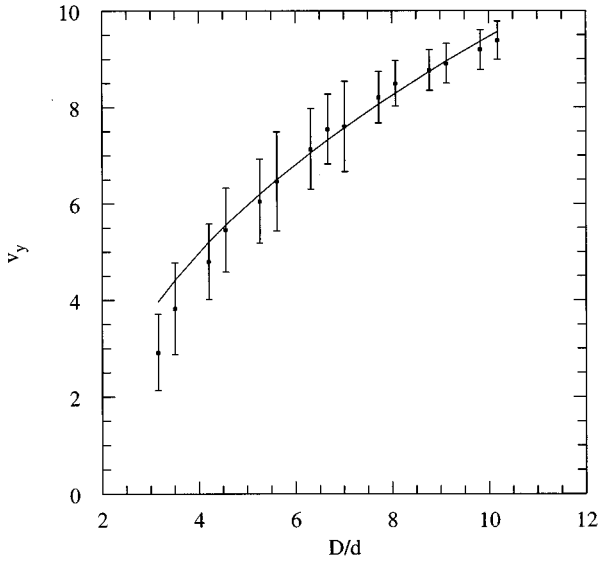

FIG. 6. Vertical outflow velocity as a function of hole size for triangular particles; the theoretical fit (using the same value of k) is shown.

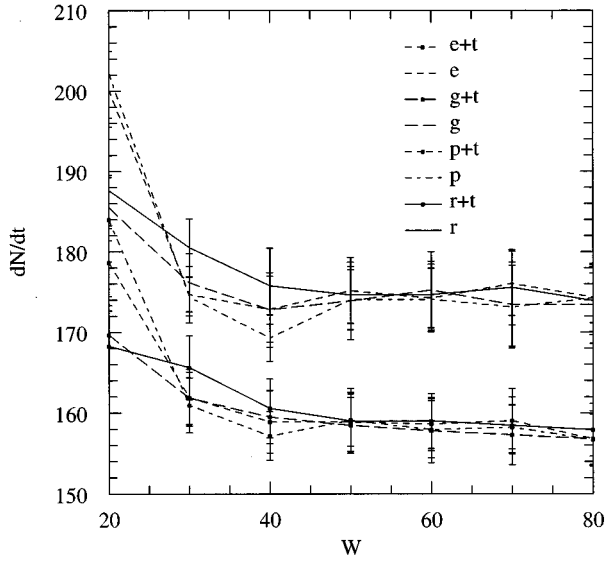

FIG. 7. Effect of container width on particle flux (for circular particles and $D=10$); the influence of different wall types (where the curve labels denote e, elastic; g, granular; p, periodic; and r, rough) and the optional inclusion of grain rotation and transverse damping (curves labeled t) is also shown.

value of k used in the fit is $k=0.71$, where, as indicated earlier, the nominal grain diameter d is defined to be the that of the circle circumscribing the triangular grain. This value is clearly an overestimate of the ill-defined effective diameter, but in view of the complex (nonconvex) grain shape any such definition must be entirely arbitrary. The fact that the effective d is overestimated explains the small value of k; experimental values [8] are typically in the range 1.3–1.5.

Figure 6 shows how the vertical outflow velocity varies with D, together with a fit to the square-root form (the flux divided by the effective aperture size) using the same value of k; the fit is once again of similar quality to that obtained for the circular grains. The horizontal flow velocity is not shown, but a linear fit also seems to work here. In each case the fit excludes the smaller holes with $D/d<5$.

B. Effect of container width

From the computational point of view, a smaller container width W reduces the work required because the system itself can be made smaller. Experimentally, as we indicated earlier, it is necessary to have $W>2.5D$ (in addition to $W>D+30d$) for the effect of the walls on the discharge rate to be negligible, but since these are little more than rules of thumb, they should not be relied upon for simulation work without further examination.

We have therefore carried out a series of measurements, using circular grains and the continuous flow approach, to investigate the W dependence of the outflow for a particular hole size $D=10$. For each value of W the total number of grains is chosen to ensure the same value of the material head H; the reason for this is to eliminate any residual H dependence from the results (see below).

The physical properties of the walls can also change the way in which they influence the flow. In order to determine the magnitude of this effect we replaced the granular sidewalls by the other kinds of boundaries enumerated earlier, namely randomly rough walls, elastic (reflecting) walls, and no sidewalls at all, i.e., periodic boundaries. Another aspect of the model is also examined in this series of measurements, namely, the influence of grain rotation and the associated transverse damping forces; since there have been granular simulations in the past that excluded rotational motion (an omission that is not readily justified for circular, or near-circular grains), it is interesting to examine how this additional degree of freedom modifies the behavior.

In Fig. 7 we summarize the results of these measurements. The widest system has $N=4000$ particles and width $W=80$, while for smaller W the value of N is proportionally lower; other details remain the same as before. The results show that the mass flux increases as W becomes smaller because stationary sloping piles on either side of the hole are less readily formed, and that because of their ability to absorb some of the stress, rough walls (more so the granular walls, with their additional protrusions) tend to reduce the flow. The influence of the walls drops to a negligible level when the system is sufficiently wide, typically for $W>4D$; the rule of thumb therefore appears to be a reasonable, though perhaps slightly optimistic approximation for MD systems. As might be expected, eliminating the tangential damping force increases the flow rate, since grains are able to slide over one another, rather than being forced to roll, which has the effect of increasing the resistance to shear flow.

C. Effect of material head

For a sufficiently large head ($H>2.5W$), granular flow is known to be independent of the total height of the bulk material (the hourglass effect). The obvious, and well-known, implication is that the pressure ceases to be depth dependent (the depth dependence close to the upper surface initially grows exponentially—the original analysis is due to Janssen; see Ref. [5]), which means that the sidewalls bear most of

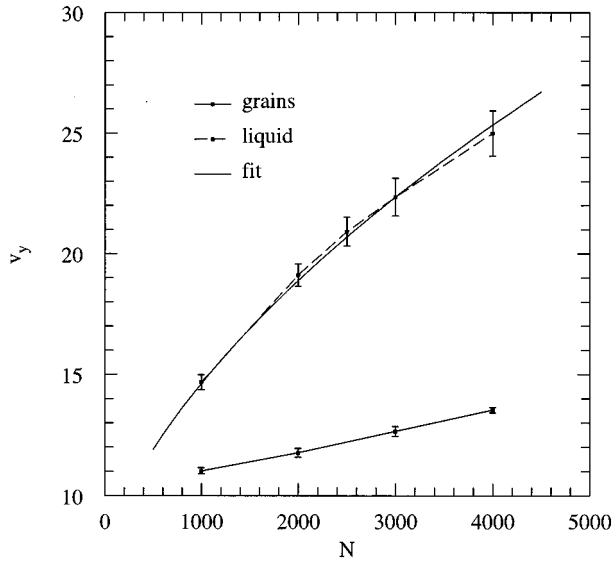

FIG. 8. Vertical outflow velocity as a function of system size for circular particles (in all cases N is chosen so that $W=50$); the results from a simple liquid simulation, as well as a fit to the theoretical result (see text), are included for comparison.

the vertical load. In this respect granular materials differ strongly from liquids, where the load on the sidewalls acts in the normal direction; the reason for this difference is the presence of static frictional forces. In the present models, as in other models used for granular simulation, the kind of static friction that inhibits the tendency to slide is absent; the viscous damping and/or elastic—actually gluelike—restoring forces that are incorporated in these models serve only to impede any sliding motion that has already started, and therefore do not provide completely adequate substitutes for static friction. Thus an important question is the degree to which the present models are able to reproduce the absence of head dependence; the same question can of course also be asked of other granular models reported in the literature.

Figure 8 shows the dependence of the vertical outflow velocity on system size for circular grains. Since the container width is the same in all cases (here $W=50$), the property measured is the dependence of the velocity on the head itself; this shows a very slow increase, far slower than the square-root dependence of a normal liquid, which is also shown for comparison, but not the strict height-independent behavior of a real granular material. The triangular model exhibits a similar behavior. The liquid results show a square-root dependence of the form $v=\sqrt{c_1H+c_2}$ (a fit is included in the figure), where the additive constant is due, in part, to the nonzero mean flow speed at the upper surface. (For the $N=2000$ system, the actual measured height of the surface is approximately 25 units.)

This result provides a clear indication that pressure varies with depth. The pressure can also be examined directly: Fig. 9 is a contour plot of the pressure variation throughout the system under steady flow conditions, for a system of circular grains with $W=50$, $N=4000$, and a hole size $D=10$. If the horizontal pressure variations that are a consequence of flow (the behavior very close to the walls is an artifact of the spatial coarse graining required for the measurements) are ignored, the vertical dependence turns out to have the hydrostatic linear form. In this respect the model does not capture the nature of a granular material.

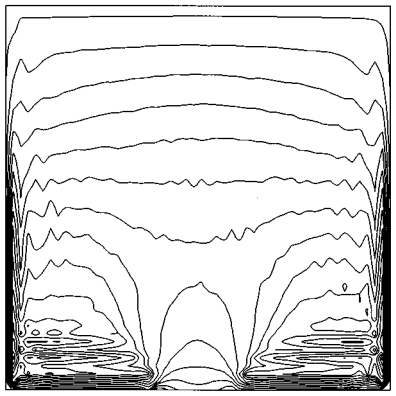

FIG. 9. Pressure distribution for circular particles: the plot extends vertically from just above the material to the level of the base, and the contour levels are evenly spaced; pressure increases almost linearly with depth, but then drops as the hole is approached.

A similar result holds even when there is no flow, as shown (for circular grains) in Fig. 10. Here pressure estimates based both on the virial pressure definition and on direct measurement of the horizontal force acting on the wall are shown for several container widths W; each result is the average of five runs during which the grains are allowed to come to rest at the bottom of the container before any measurement is made (the runs use different random initial conditions). The total numbers of grains are chosen so that the systems all have essentially the same material head. For narrower systems, the pressure does not increase so rapidly with depth; some of the vertical load is carried by the sidewalls owing to the way the material is forced to pack in the relatively narrow space available. There are large variations between individual runs because the results correspond to zero

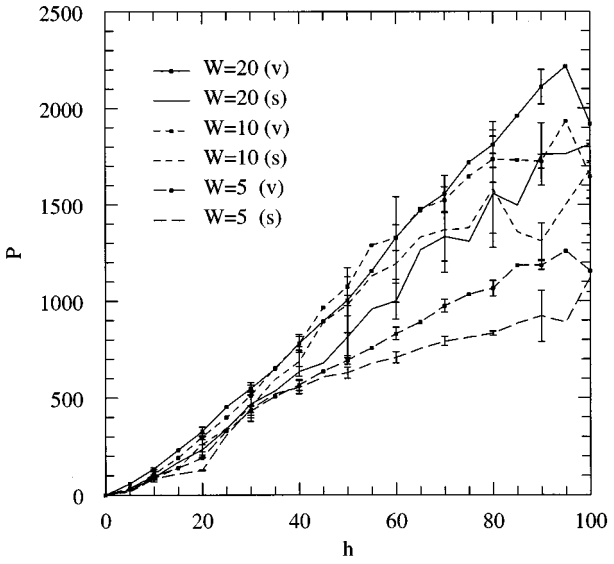

FIG. 10. Depth dependence of pressure for the circular particle system at rest (h is the distance from the upper surface), with the error bars reflecting the spread of values over separate runs; both virial (labeled v) and direct sidewall measurements (s) are shown.

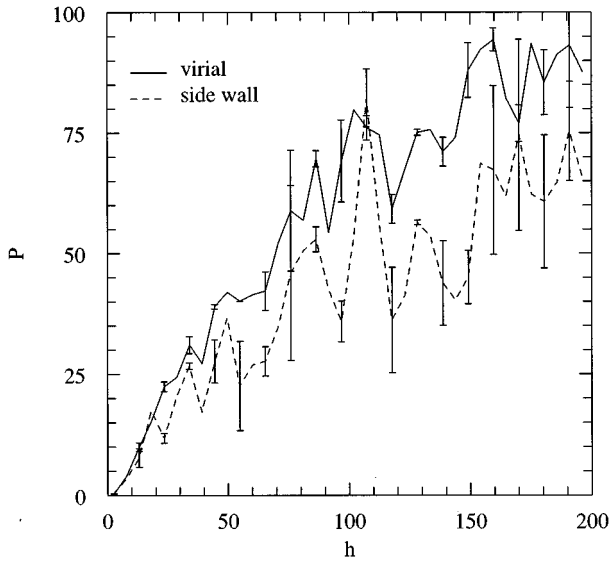

FIG. 11. Pressure depth dependence in a narrow ($W=16$) system of triangular particles at rest; the deviations from linearity are substantial.

temperature and are not self-averaging.

The corresponding series of measurements for the triangular model reveals similar behavior. Only one example is shown here: Fig. 11 shows the behavior for a narrow container with $W=16$, a width just over five times the grain diameter (the large error bars are an indication of the variation between runs). Overall, the departure from linearity is slightly stronger than for circular grains, as are the differences between the bulk (virial) and wall pressure results. The difference is at least partly due to the way the triangular grains pack at the bottom of the container: direct observation of the grain configurations suggests that the dovetailed structures that form (horizontally adjacent grains pack with alternating directions) are, to some extent, self-supporting, and so do not place as large a horizontal load on the sidewalls as the simpler circular grains. The fact that the pressure grows at a less than linear rate suggests that the rough sidewalls begin to carry a portion of the vertical load. Here too, it is the absence of static friction that is responsible for the inability to correctly reproduce this aspect of granular behavior.

This failure to achieve full depth independence is not confined to the present models. A model which does include friction [7] (the often-used spring-based mechanism, not true static friction) shows very similar behavior: the flow velocity is weakly head dependent, and the vertical load distribution is supported entirely by the base of the container, with no assistance from the side walls. The latter feature corresponds to the behavior of a hydrostatic system. Corresponding measurements for other models have not been reported in the literature, although they are unlikely to differ significantly.

D. Stress distribution

Much of the unusual behavior of granular materials (in comparison with liquids) is attributed to the formation of archlike structures that are able to redistribute the stress, transfer the load to the side walls, and impede the flow of material through the hole [8]. This aspect of the behavior can

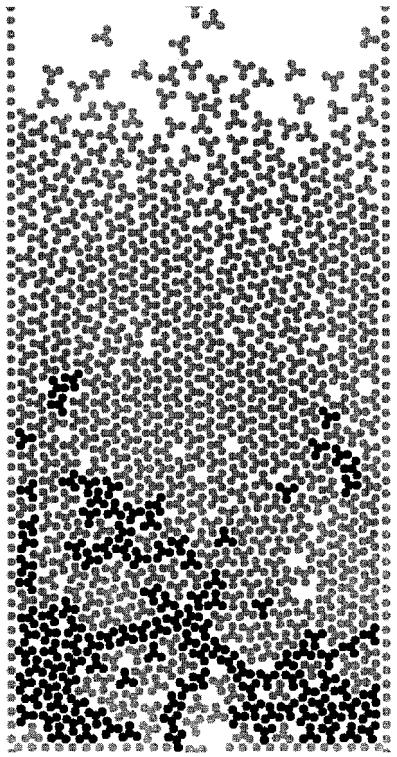

FIG. 12. Snapshot showing regions of instantaneous high stress (the grain recycling mechanism differs from that used for the measurements—see text); grains that are subject to stress (computed from the virial) more than 60% above average are colored black.

be examined directly by means of computer graphics. In Fig. 12 we show an example of the stress distribution. Note that the recycling mechanism used here differs slightly from that considered elsewhere in this paper in that grains are not repositioned after falling through the hole; instead, the vertical coordinate is merely subject to a periodic boundary condition. Grains that experience an instantaneous stress value (the value of the virial computed for that grain) exceeding the overall average by 60% or more are shown in black.

While the stress patterns vary greatly across a sequence of such images, what stands out in these pictures is the nonuniform nature of the stress distribution and the appearance of filamentlike zones of high stress (similar behavior can be observed with circular grains). These flickering arches are the MD equivalent of the mechanism proposed to explain what occurs in real granular flow; an example of the force network that occurs in controlled experiments appeared in Ref. [22]. The absence of static friction prevents the arches from playing a more prominent role in redistributing stress since they are unable to provide a load-bearing network spanning the gap between the vertical sidewalls except, possibly, in the very narrowest of the systems examined.

Given the nature of the stress distribution, it is not difficult to resolve the apparent paradox between the fact that while the flow dependence on hole size resembles that of a granular material, the vertical pressure variation is essentially that of a normal liquid. Hole flow involves a particular type of local behavior in the neighborhood of the opening: the models used here are able to produce the kinds of stresses

needed to form—at least in a statistical sense—the small archlike structures [8] that are responsible for retarding the flow, leading to the characteristic $\frac{3}{2}$ power-law dependence on hole size [Eq. (2)]. The hydrostatic aspect of the behavior results from the inability to form static arches that would create the load-bearing network; this is the only way to transfer vertical load to the sidewalls and thereby reduce, or eliminate, the pressure growth in the interior. Only true static friction, an effect difficult to incorporate into the model (with the possible exception of a considerably more complex model for individual grains [19]), can account for this behavior.

E. Motion of individual grains

The detailed motion of individual grains is difficult to measure experimentally, especially in three dimensions. There has been some recent work [4] involving what amounts to a two-dimensional experiment and a comparison with simulation, but this deals with chute flow rather than aperture flow. Because of the complex nature of the observed motion, which includes cooperative rotation and distortion of blocks of grains, it is difficult to quantify the behavior in a meaningful way.

Simulations of aperture flow incorporating real-time graphics (not shown here) reveal the formation of transient domains that shear and rotate in a manner reminiscent of the experimental observations mentioned above (that were for a different class of flow problem), as well as a streaming flow whose path exhibits a noticeable degree of time-dependent meandering. A snapshot showing the triangular grain (center-of-mass) trajectories followed over a short period of time appears in Fig. 13 (this demonstration is based on the same grain recycling mechanism used in Fig. 12). In this picture, not only is the fact that motion is strongest near the hole apparent (ignoring the motion near the top surface), but the meandering nature of the flow can also be seen. If the particle trajectories are followed over longer intervals the flow patterns are seen to shift gradually in unpredictable ways. Further visual information about the vertical motion and rotation of domains can be observed by ''painting'' the grains in different colors based on their heights at a given instant, and then monitoring how the initial color stripes change with time.

If the short-term, time-dependent behavior is averaged out of the results, then much of the flow behavior can be condensed into contour plots of the translational and rotational kinetic energy, shown respectively in Figs. 14 and 15. These results are for circular grains, but the triangular grain results are essentially the same. The region where the flow is most developed is clearly delineated, and the relatively high angular velocity that occurs near the edges of the hole is also apparent. These graphs confirm that the motion is dominated by what occurs in a central funnel-shaped region of the container, and that grains move faster as they approach the hole; rotational motion accompanies the shear at the funnel boundaries, but is most pronounced for those grains exiting close to the edges of the hole.

F. One-pass flow

The two previous studies of this particular granular flow problem [6,7] both considered only a single pass of the material through the hole. The latter involved a sufficiently large (but narrow) system to ensure a prolonged measurement period, but in the former the behavior was essentially transient throughout.

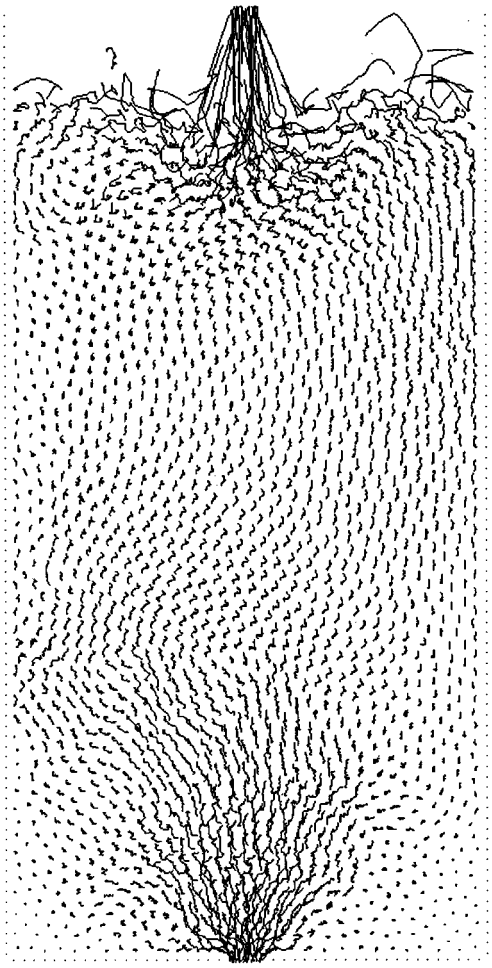

FIG. 13. Triangular grain trajectories followed over a short time interval; the meandering nature of the trajectories changes unpredictably with time (see text).

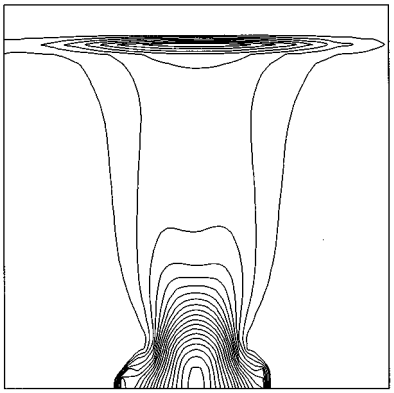

FIG. 14. Translational kinetic-energy distribution for circular particles (note that the hole is located a small distance above the bottom of the figure); since the contour levels are evenly spaced, starting from just above zero, it is clear that away from the hole the average grain speed is very low (the increase at the top reflects the behavior of incoming grains).

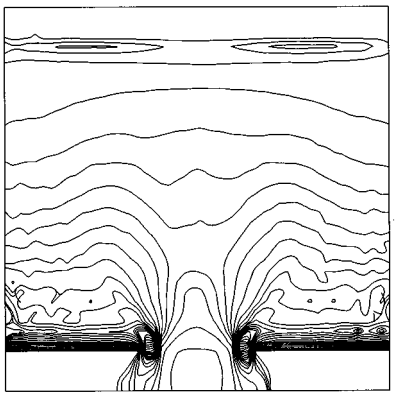

FIG. 15. Rotational kinetic-energy distribution (circular particles); rotation is most pronounced for grains leaving the container close to the hole edges.

The results described in this section are for a system in which circular particles make a single pass through the hole. The principal reason for this calculation is to establish that the slightly different model used in the present series of studies does indeed display similar time-dependent behavior to the one studied previously [6], in which a Hertzian overlap interaction was used rather than the functional form employed here. The simulation was carried out for a system having the same dimensions as before, namely $N=2500$ grains, flowing out from a container of width $W=50$ (in terms of the reduced units defined earlier).

The graphs of the time-dependent particle flux for different hole sizes D (not shown here) appear to have a common overall shape, and this suggests that a display of suitably scaled results might prove informative. Figure 16 shows the time-dependent flux for several D values. Since the continuous flow analysis demonstrated that flux varies as $D^{3/2}$ (ignoring the correction due to the empty annulus), the flux has been multiplied by $D^{-3/2}$, and the time axis suitably scaled to preserve the area under the curves. The degree of overlap

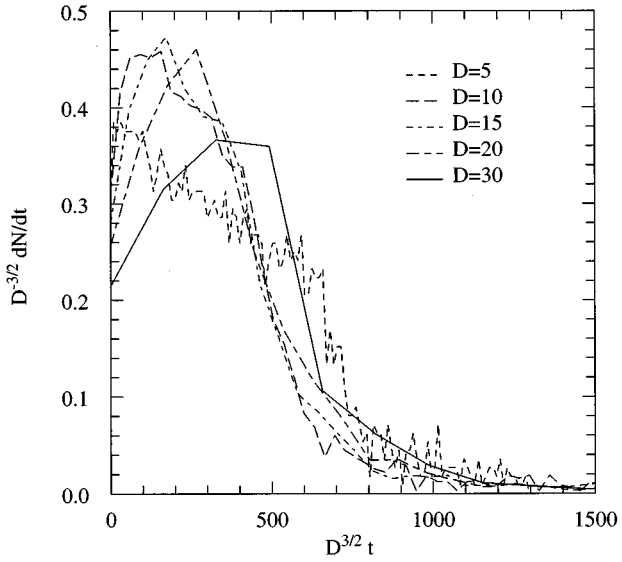

FIG. 16. Single-pass flow: scaled particle flux as a function of scaled time for different hole sizes D.

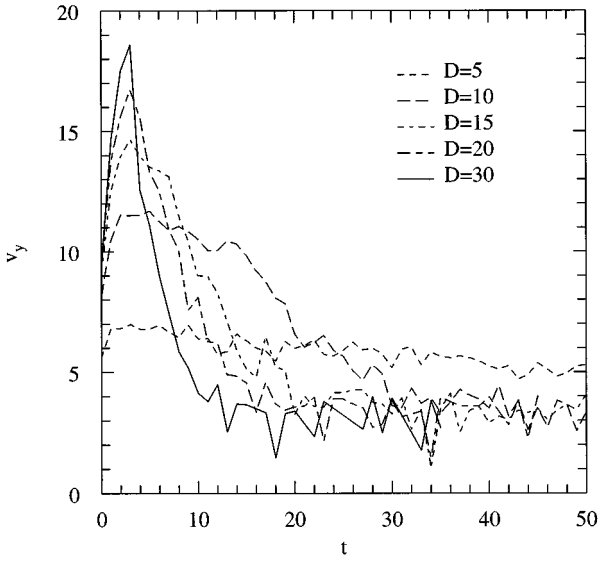

FIG. 17. Single-pass flow: vertical outflow velocity as a function of time for different hole sizes.

of the different curves offers a hint of a universal shape, provided the hole is neither so small ($D\leqslant 5$) that the theoretical result no longer applies, nor too large ($D\geqslant 30$) for the granular arching mechanism across the hole to be able to function (or a hole whose edges come too close to the walls). The question whether this implies the existence of true scaling, or merely reflects a numerical coincidence, awaits further analysis. The time-dependent vertical component of the outflow velocity is shown in Fig. 17; no obvious scaling behavior is apparent in this case.

From the measurements of the scaled discharge rate and vertical flow velocity, as well as from a series of snapshots of the grain positions and trajectories (not shown), it is apparent that there are two flow regimes. Most of the grains flow out during the early stage of the run; these are the grains located in the central wedge-shaped region over the hole which are able to flow out directly. The flow during the latter part of the run involves grains that roll down the sloping heaps that have formed against the container walls; here the flow rate is strongly reduced due to the retarding effect of the shear forces that compel the surface grains to roll rather than slide. The horizontal flow velocity component (not shown) is consistent with this behavior; initially it is small, but the value increases after the drop in vertical velocity has occurred. These results are qualitatively similar to those reported in the earlier work [6].

V. SUMMARY AND CONCLUSIONS

In this paper we have described a series of two-dimensional simulations of granular flow through a horizontal aperture, a model for discharge from a storage silo. The approach differs in one important respect from previous studies of this problem in that the grains are recycled after exiting through the hole. This permits the extended measurements under conditions of constant material head that are essential for obtaining accurate estimates of the mean flow.

Two types of models have been studied. One involves grains that are circular in shape and incorporates both normal

and transverse frictional damping forces; the former force ensures energy dissipation, while the latter reduces the ability of particle layers to slide over one another. The second of the two models is based on grains with a complex shape chosen to inhibit rotation. The presence of substantial indentations along the grain edges serves to encourage interlocking; this, in turn, tends to inhibit sliding motion. This complex grain geometry also captures another feature of real granular matter insofar as a certain amount of dilation is necessary before flow can begin. The simulations demonstrate that these two very different models of granular materials yield similar results.

The functional dependence of the flow rate on the hole width has been shown to be very close to (the two-dimensional version of) the theoretical result proposed in order to explain the experimental observations. In this respect, transverse forces acting between circular grains are equivalent to the interlocking effects of the triangular grains. The influence of various kinds of sidewalls on the flow has been explored for circular grains, as has the effect of removing the transverse damping and the concomitant rotational motion. Spatial kinetic-energy distributions have been used to demonstrate where the grain motion—both translational and rotational—is concentrated.

The residual dependence of flow rate on material head is far weaker than the corresponding hydrodynamic result for both circular and triangular models, but the fact that some dependence remains, as well as the depth-dependent pressure, are indications that although both models can describe the flow correctly (for a given material head), they are unable to account for other aspects of granular behavior. While pressure should initially grow exponentially with depth and rapidly achieve a constant, depth-independent value, what is observed, both here and in previous simulation work, is that the pressure continues to increase with depth in a near-linear manner. (It remains to be seen whether the situation is improved in three dimensions, where the surface to volume ratio is larger.) For narrower containers, however, the pressure grows at a slower rate, an indication that the rough sidewalls are beginning to carry at least part of the vertical load.

A plausible explanation for the fact that the models are able to capture certain aspects of granular behavior, but not others, is that different properties depend on distinct features of the interactions between grains. Obtaining the correct pressure (or stress) is crucially dependent on the ability to model the influence of static friction, a factor not accounted for in current granular simulations because of the difficulty in constructing suitable dynamical models. On the other hand, the damping forces governing the flow of circular grains appear to provide an effective representation of the way irregular grain shape and dynamical friction forces influence the overall granular motion. The triangular grains, which provide a simplified representation of the granular asperities that tend to inhibit transverse motion, provide an alternative—and in a sense more realistic—means for modeling the behavior, with a very similar outcome.

ACKNOWLEDGMENTS

This research was supported in part by a grant from the Israel Science Foundation.

[1] G. C. Barker, in *Granular Matter: An Interdisciplinary Approach*, edited by A. Mehta (Springer, Heidelberg, 1994), p. 35.
[2] H. J. Herrmann, in *3rd Granada Lectures in Computational Physics*, edited by P. L. Garrido and J. Marro (Springer, Heidelberg, 1995), p. 67.
[3] H. M. Jaeger, S. R. Nagel, and R. P. Behringer, Rev. Mod. Phys. **68**, 1259 (1996).
[4] T. G. Drake and O. R. Walton, J. Appl. Mech. **62**, 131 (1995).
[5] R. M. Nedderman, *Statics and Kinematics of Granular Materials* (Cambridge University Press, Cambridge, 1992).
[6] G. H. Ristow, J. Phys. (France) I **2**, 649 (1992).
[7] P. A. Langston, U. Tüzün, and D. L. Heyes, Chem. Eng. Sci. **49**, 1259 (1994).
[8] R. M. Nedderman, U. Tüzün, S. B. Savage, and G. T. Houlsby, Chem. Eng. Sci. **37**, 1597 (1982).
[9] W. A. Beverloo, H. A. Leninger, and J. van der Velde, Chem. Eng. Sci. **15**, 260 (1961).
[10] A. Harmens, Chem. Eng. Sci. **18**, 297 (1963).
[11] O. R. Walton, in *Numerical Simulation of Two-Phase Flow*, edited by M. C. Roco (Butterworth-Heineman, Stoneham, MA, 1993), p. 239.
[12] J. Schäfer, S. Dippel, and D. E. Wolf, J. Phys. (France) I **6**, 5 (1996).
[13] P. A. Cundall and O. D. L. Strack, Geotechnique **29**, 47 (1979).
[14] O. R. Walton, in *Mechanics of Granular Materials*, edited by J. T. Jenkins and M. Satake (Elsevier, Amsterdam, 1983), p. 327.
[15] C. S. Campbell, Annu. Rev. Fluid Mech. **22**, 57 (1990).
[16] J. A. C. Gallas and S. Sokolowski, Int. J. Mod. Phys. B **7**, 2037 (1993).
[17] T. Pöschel and V. Buchholz, Phys. Rev. Lett. **71**, 3963 (1993).
[18] J. M. Ting and B. T. Corkum, J. Comp. Civ. Eng. **6**, 129 (1992).
[19] T. Pöschel and V. Buchholz, J. Phys. (France) I **5**, 1431 (1995).
[20] G. H. Ristow and H. J. Herrmann, Physica A **213**, 474 (1995).
[21] D. C. Rapaport, *The Art of Molecular Dynamics Simulation* (Cambridge University Press, Cambridge, 1995).
[22] O. Pouliquen and R. Gutfraind, Phys. Rev. E **53**, 552 (1996).